

Radiated Measurements of an Ultrawideband Surveillance Radar

Robert T. Johnk¹, Frank H. Sanders, Kristen E. Davis, Geoffrey A. Sanders, John D. Ewan, Ronald L. Carey

*Institute for Telecommunication Sciences (NTIA/ITS)
325 Broadway, Boulder Colorado USA 80305*

¹ bjohnk@its.bldrdoc.gov

Steven J. Gunderson²

*Naval Facilities Engineering Command
Port Hueneme, California USA 93043*

² steve.gunderson@navy.mil

Abstract— We provide detailed descriptions of recent radiated emissions measurements conducted by the National Telecommunications and Information Administration (NTIA) Institute for Telecommunication Sciences (NTIA/ITS) in Boulder, Colorado. ITS engineers performed a comprehensive series of radiated emission measurements on the Shore-Line Monitoring System (SLiMS). The SLiMS system is currently being developed by Time-Domain Acquisition Holdings® (TDC) under the sponsorship of the Naval Facilities Engineering Command (NAVFAC). The measurement results demonstrate both low emission levels, consistent with existing U.S. electromagnetic compatibility requirements and a low potential for causing interference to incumbent systems. A high level of precision is required to perform the characterization.

I. INTRODUCTION

The United States is currently facing increasingly significant threats; dangers to U.S. personnel and assets have increased both overseas and at home. The U.S. Department of Defense (DOD) needs to use surveillance radars to detect and identify intruders on the ground. These systems must be compatible with incumbent electronic systems and minimize safety hazards to other equipment or personnel. In order to ensure safe operation compliance with existing electromagnetic compatibility requirements, the radio-frequency emissions characteristics of these surveillance systems must be thoroughly understood. The Institute for Telecommunication Sciences of the National Telecommunications and Information Administration (NTIA/ITS) possesses a unique combination of engineering expertise, equipment, and facilities to measure and evaluate the radio-frequency (RF) performance of these systems.

The Naval Facilities Engineering Command (NAVFAC) is sponsoring the development of an ultrawideband (UWB) radar fence that can detect, track, and classify intruders, the Shore-Line Intrusion Monitoring System (SLiMS). The radar consists of a distributed system of autonomous transmit/receive modules mounted on poles that are deployed around the perimeter of a facility to be protected. The number of poles and modules varies depending on the coverage needed. There are currently plans to operate SLiMS at

Whidbey Island Naval Air Station, Washington, to provide perimeter security. The U.S. Department of Energy (DOE) is currently experimenting with SLiMS at one of its facilities.

At the request of NAVFAC, NTIA/ITS engineers performed a comprehensive set of emissions measurements on a shortened pole structure containing a single radar module [1]. NAVFAC wants to ensure that emission levels from their system fall below NTIA and Federal Communications Commission (FCC) UWB radiated emissions limits and that their system operates safely. NTIA/ITS coordinated with electromagnetic compatibility (EMC) engineers at the Naval Surface Warfare Center (NSWC) in Dahlgren, Virginia to confirm that the system does not constitute an electromagnetic radiation hazard to either personnel (HERP) or ordinance (HERO).

II. RADIATED EMISSIONS TEST SETUPS

ITS engineers carried out a series of radiated measurements inside a fully anechoic chamber located at the NTIA/ITS laboratories in Boulder, CO. The chamber testing configuration is shown in Fig. 1. It was composed of a SLiMS short pole mounted on a moveable cart, a multiple-axis positioner, and a fixed receiving system. The receiving system included an antenna mounted on a fiberglass pole which, in turn, fed a signal to either an oscilloscope or a spectrum analyzer. The feed network had two coaxial cables connected in series with a low-noise amplifier (LNA). The separation, D , between the transmitting and receiving antennas varied from 2–4 m.

We used two different receiving antennas. The first was an Antenna Research® (ARA)¹ parabolic dish with a log-periodic dipole array feed shown in Fig. 2. The antenna had a

¹ Certain commercial equipment, materials, and/or programs are identified in this report to specify adequately the experimental procedure. In no case does such identification imply recommendation or endorsement by the National Telecommunications and Information Administration, nor does it imply that the program or equipment identified is necessarily the best available for this application.

diameter of 91 cm and a manufacturer-specified frequency range of 1–18 GHz. We also used an Electrometrics® dual-ridged horn (DRH) antenna shown in Fig. 3, which also had an operational frequency range of 1–18 GHz. We used the two antenna types to cross-check our emissions measurements and to verify far-field conditions. However, the majority of radiated measurements were performed using the dish antenna due to its higher gain.

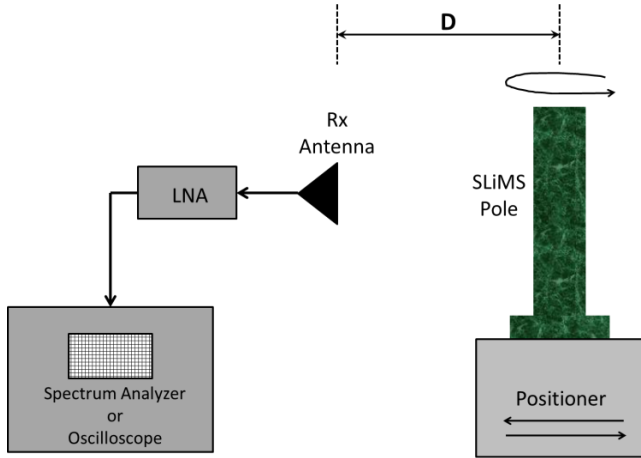


Fig. 1 Test setup for radiated emissions measurements.

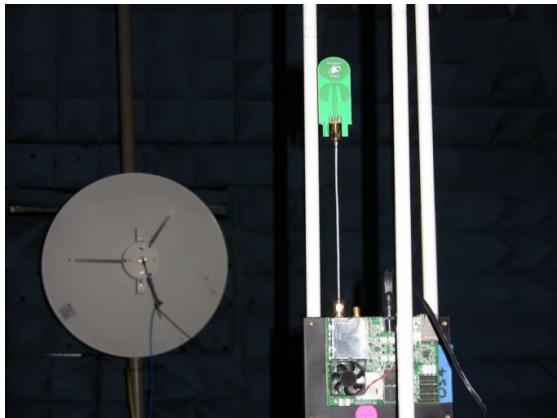


Fig. 2. P400 UWB radar and parabolic dish receiving antenna.

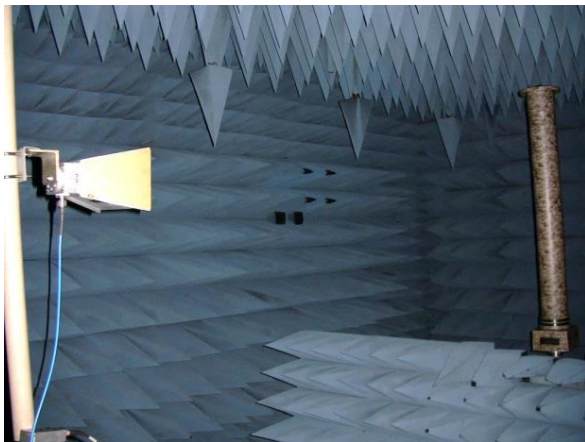


Fig. 3. SLiMS pole 3 m emissions measurement setup with a DRH receiving antenna with a 3 mm thick camouflaged PVC® radome.

On the transmitting side, we installed the P400 radar inside a shortened SLiMS pole and placed it on a moveable cart with a multiple-axis antenna positioner. We used two different deployments: 1) an off-center configuration and 2) a centered configuration. The off-centered configuration, shown in Fig. 2, consisted of a straight section of semi-rigid coaxial cable connected directly to a printed-circuit antenna. Due to the combination of the straight cable and the position of the transmitting port, the antenna was displaced 3.5 cm away from the geometric center of the SLiMS short pole. Since the off-center configuration exhibited significant pattern asymmetries, we also deployed the antenna in the centered configuration shown in Fig. 4. In this case, we used a bent section of semi-rigid cable to connect the P400 to the antenna element. The outer surface of the interconnecting cable was also covered with an EMI-suppressing dielectric material to reduce common-mode currents and to maintain better pattern control. This centered configuration provided improved pattern symmetry.



Fig. 4. Centered antenna configuration.

III. MEASUREMENT INSTRUMENTATION

We used three instruments in the radiated emissions measurements [1]:

- A spectrum analyzer
- A high-speed real-time digitizing oscilloscope
- A vector network analyzer for feed line and antenna calibrations

We used both the spectrum analyzer and the oscilloscope, shown in Fig. 5 to receive the radar signals. The spectrum analyzer was used for the majority of the measurements because of its precision and high dynamic range. We performed swept-frequency measurements, pattern measurements, and zero-span measurements. The spectrum analyzer settings were identical to those used in the conducted measurements. We used the oscilloscope in a more limited role to capture full-bandwidth time-domain waveforms and to verify the time-domain structure of the emitted waveforms.

We used the vector network analyzer (VNA) shown in Fig. 5 to measure the insertion gain of the receiving antenna feed network that included two cables and the LNA. The VNA data

allowed us to convert the spectrum analyzer power readings directly to the transmitted effective isotropic radiated power (EIRP) levels. We also used the VNA to perform the three-antenna calibration, the details of which are given in [1].

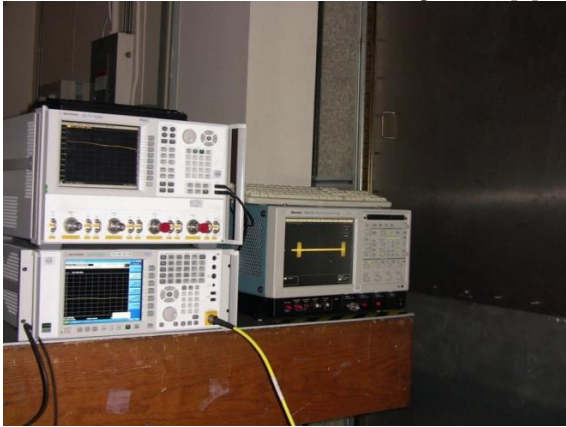


Fig. 5 Test instrumentation for the radiated emissions measurements. The oscilloscope is located on the right, and the spectrum analyzer is on the bottom left. The vector network analyzer is located on the top left.

IV. TIME-DOMAIN WAVEFORMS

A thorough understanding of the time-domain character of the radar waveform is necessary for the correct measurement of its spectrum properties. We used a high-speed oscilloscope with the setup shown in Fig. 1 to measure the full-bandwidth waveform characteristics of the P400 radar. We captured two waveforms using both a high-speed and a slower-speed sampling rate. The first record was 40 μ s long and sampled at a rate of one sample per 0.625 ps in order to capture fast events and fine detail. Fig. 6 shows the fundamental wavelet that was captured in this mode.

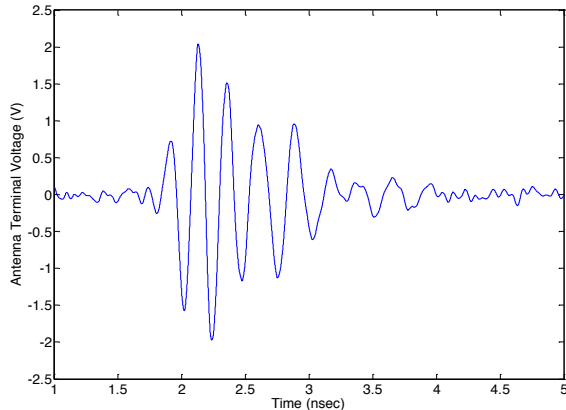


Fig. 6. Single wavelet emitted by the by the SLiMS short pole received by the dish antenna at $D = 3$ m.

The wavelet is an oscillating sinusoid with variable amplitude and a downward chirp in frequency. The wavelet duration is approximately 2.2 ns. Fig. 7 depicts two successive wavelets captured in the high-speed mode. The wavelets have a time separation of approximately 57.5 ns between them. We then acquired a much longer 400 ms record at a sampling interval of 0.2 μ s in order to capture the global macroscopic

behavior of the waveform. At this interval, the waveform was under-sampled, but its macroscopic characteristics were discernible. Fig. 8 depicts two complete P400 bursts, each of which contains approximately 400,000 wavelets. The duration of each burst is 24 ms, and time separation between the bursts is 0.265 seconds. It was this large-scale waveform burst behavior that dictated the spectrum analyzer settings.

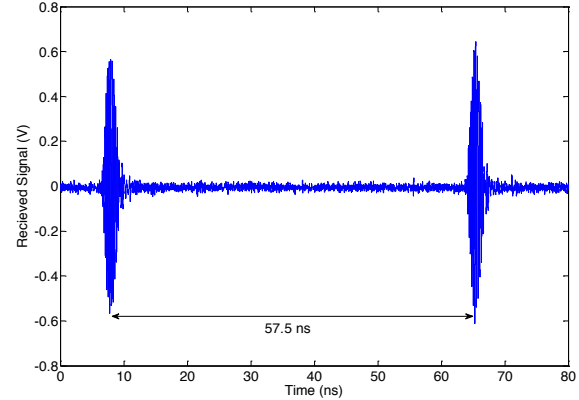


Fig. 7. Two successive wavelets emitted by the SLiMS short pole received by the dish antenna at $D = 3$ m.

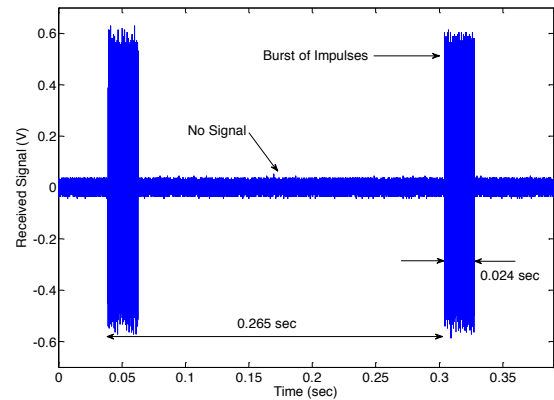


Fig. 8. Radiated burst of the SLiMS pole received by the dish antenna at $D = 3$ m.

We did consider trying to capture a full-fidelity P400 burst using the oscilloscope. However, capturing a 24 ms segment at one sample per 0.625 ps would have greatly exceeded the memory capacity of the oscilloscope. We therefore concentrated on the capture of partial records to understand the key waveform parameters and global waveform structure.

V. SPECTRUM ANALYZER SETTINGS

We carried out a series of radiated measurements using an Agilent 9030A PXA signal analyzer. We configured it to operate in the spectrum analyzer mode and to perform swept-frequency measurements over selected frequency ranges. We used both peak and average detection for our measurements. In order to assess interference potential to a wide variety of systems we measured at five different RBW's: 0.1, 0.3, 1, 3, and 8 MHz. We configured the instrument to capture two bursts within each frequency bin during a sweep. This

required a dwell time of 0.53 s per frequency bin during the sweep. Table 1 summarizes the required sweep times for various RBWs. The sweep time is computed from the formula

$$\text{Sweep Time(sec)} = \frac{\text{Frequency Span (MHz)}}{\text{RBW (MHz)}} \times 0.53$$

This result is based on a burst interval of 0.265 s and measuring two bursts in each frequency bin. The spectrum analyzer measures up to 40,000 frequency bins, and it has a maximum sweep time of 4,000 s. This sweep time limitation made it necessary in some cases to subdivide the measurements into either two or four bands, depending on the range of frequencies needed.

TABLE 1. SPECTRUM ANALYZER SWEEP TIMES

Resolution Bandwidth	Frequency Range (MHz)	Number of Frequency Bins	Sweep Time (sec)
100 kHz	3000–5000	20000 (4 bands)	10600 (4 bands)
300 kHz	3000–5000	6667	3533
1 MHz	3000–5000	2000	1061
1MHz	1000–15000	14000 (2 bands)	7420 (2 bands)
3MHz	3000–5000	667	354
3 MHz	1000–15000	4667	2474
8 MHz	3000–5000	250	133
8 MHz	1000–15000	1750	930

VI. COMPUTING EIRP FROM SPECTRUM ANALYZER READINGS

The key parameter in the radiated emissions was the EIRP. The EIRP was computed from the measured spectrum analyzer data using the seven-step process shown in Fig. 9. The steps incorporated a combination of both calibration corrections and theoretical calculations. The process started with the measured spectrum analyzer data. The feed network calibration was applied and the voltages were calculated at the output port of the receiving antenna. We used the antenna factor calibration data to infer the incident electric field at the antenna aperture plane. Next, we calculated the plane-wave electromagnetic power density at the aperture plane from the electric field values. In the final step, we multiplied the power density by the surface area of sphere of radius D, the distance from the antenna aperture to the SLiMS antenna.

VII. SWEPT-FREQUENCY MEASUREMENTS

The swept-frequency measurements constitute the primary data set that we used to characterize the SLiMS radiated emissions characteristics.

In order to ensure that our measurements were in the far field, we also performed extrapolation measurements at fixed separations over the range of $2.0 \text{ m} \leq D \leq 4.0 \text{ m}$, using both the dish and the DRH antennas for reception. We used two types of receiving antennas in order cross-check our results, as well as to verify both the far-field behavior and the antenna calibrations.

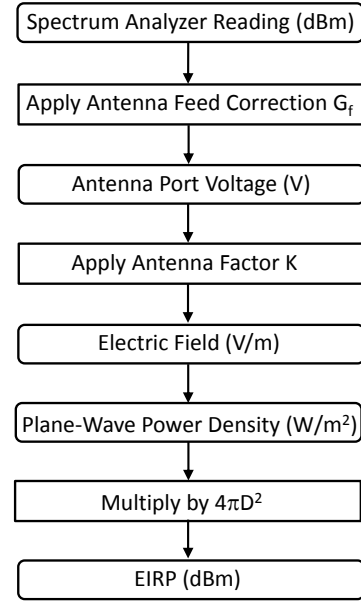


Fig.9. Flow chart for computing effective radiated power from the spectrum analyzer measurements.

Fig. 10 shows the swept-frequency measurements for average detection and the dish receiving antenna at $D = 3 \text{ m}$. We show results with $\text{RBW} = 1, 3 \text{ and } 8 \text{ MHz}$. We have included noise floor plots for these three bandwidths. The noise floor plots were obtained by turning off the radar and performing swept measurements of the background noise. The resulting noise is generated by the feed system network. The noise floor exhibits approximately a $10 \log_{10}(\text{RBW})$ behavior for both types of detection. With the radar powered up and operating, the results become noise limited somewhere in the range of 9–10 GHz. Above this range, the measurements are dominated by noise, with no visible signal components. This effect is caused by the combination of the weak UWB signal and the increased path loss between transmitter and receiver. A similar trend in signal and noise characteristics is seen when we configure the spectrum analyzer for peak detection.

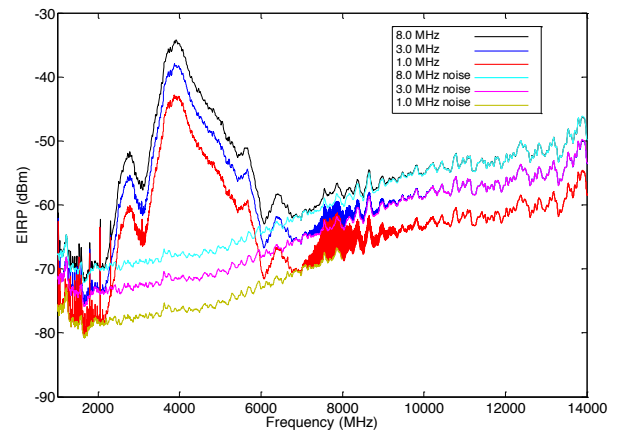


Fig. 10. Radar and noise floor measurements with a dish receiving antenna at $D = 3.0 \text{ m}$, average detection and $\text{RBW} = 1, 3, \text{ and } 8 \text{ MHz}$.

Figs. 11 depicts the peak-detected SLiMS emissions obtained over five resolution bandwidths: 100 kHz, 300 kHz, 1 MHz, 3 MHz, and 8 MHz. The corresponding average detected results are shown in Fig. 12. In the vicinity of the peak emissions, the resulting amplitudes exhibit approximately a $10 \log_{10}(RBW)$ variation for $RBW=1, 3,$ and 8 MHz. The amplitude spectra once again become “hashy” at resolution bandwidths less than 1 MHz due to the complex waveform structure of the of the SLiMS signal.

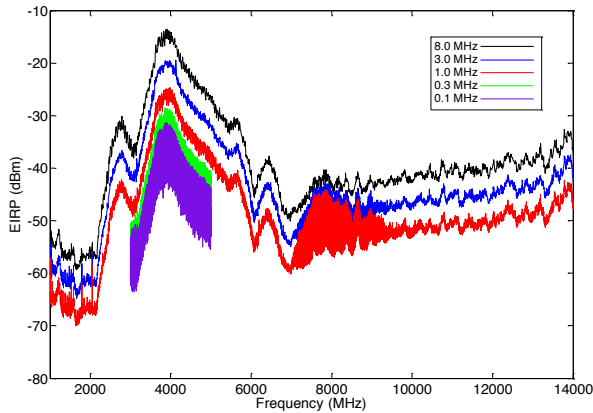


Fig. 11. Swept-frequency, P400 measurements with a dish receiving antenna at $D = 3.0$ m, peak detection and $RBW = 0.1, 0.3, 1, 3$ and 8 MHz.

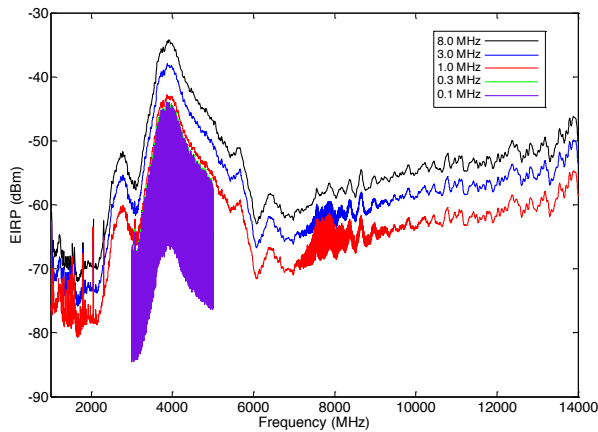


Fig. 12. Swept-frequency, P400 measurements with a dish receiving antenna at $D = 3.0$ m, average detection and $RBW = 0.1, 0.3, 1, 3,$ and 8 MHz.

VIII. EXTRAPOLATION MEASUREMENTS

In addition to the measurements at $D = 3$ m, we performed emissions measurements at 2 m and 4 m with $RBW = 8$ MHz. This was done to ensure that we were in the far field of the P400 radar.

Figs. 13 and 14 show the average-detected EIRP values for $D = 2, 3$ and 4 m for the dish and DRH antennas respectively. In the case of the DRH antenna, the EIRP results nearly overlay, which indicates that we have achieved a far-field condition with both the DRH and SLiMS antennas. We see a deviation from this condition at $D = 2$ m because the dish

antenna was not in the far field. The dish results, however, did converge at $D = 3.0$ m and 4.0 m, indicating that far-field conditions were satisfied at these separations. The results indicate that the measurement antenna was in the far field of the SLiMS transmitting antenna for all distances $D \geq 3.0$ m.

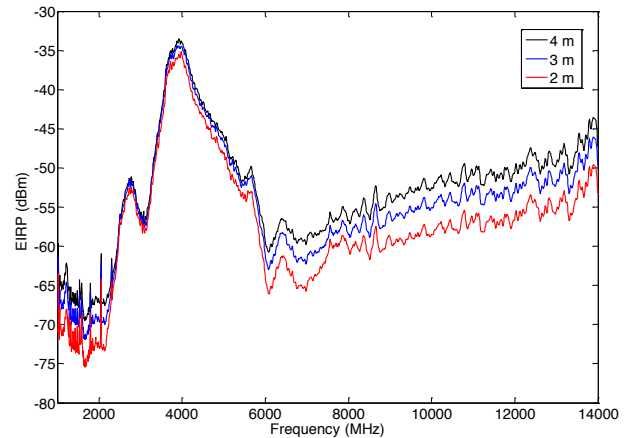


Fig. 13. Average detected EIRP ($RBW = 8$ MHz) swept-frequency results obtained at $D = 2.0, 3.0,$ and 4.0 m with a dish receiving antenna.

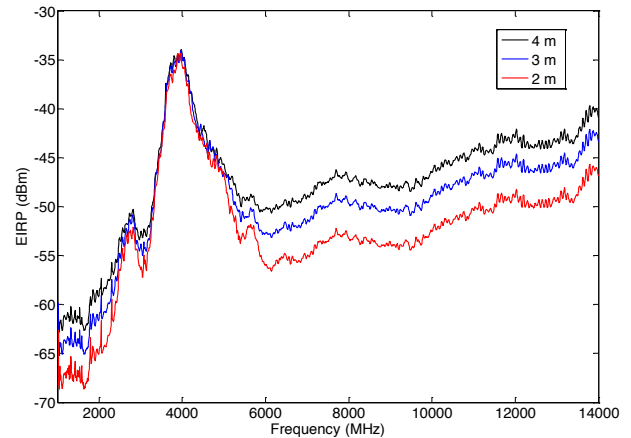


Fig. 14. Average detected EIRP ($RBW = 8$ MHz) results obtained at $D = 2.0, 3.0,$ and 4.0 m with a DRH receiving antenna.

IX. COMPARISON WITH FCC PART 15 UWB EMISSION LEVELS

We compared our swept-frequency measured data to the following NTIA- and FCC-specified limits using RMS averaging with $RBW = 1.0$ MHz as required by NTIA [2] and the FCC [3]:

- Part 15 surveillance radar emissions limits in the 1000–14000 MHz frequency range
- Part 15 limits at the GPS L1 and L2 frequencies in the 1–2 GHz frequency range
- Part 15 limits in the radio astronomy band 4990–5000 MHz

- NTIA 01-43 maximum EIRP limits and FCC Part 15 limits in the 4200–4400 MHz radar altimeter band

Fig. 15 directly compares our measured results to the FCC UWB mask for surveillance radar systems over the 1000–14000 MHz frequency range. The levels fall 2 dB or more below the limits near the emissions peak. The margins are even larger outside this frequency range. The margins are in excess of 5–10 dB throughout this frequency range. The margin seen in the radio astronomy band (4990–5000 MHz) is greater than 14 dB. The SLiMS system emissions fall comfortably below these limits. The UWB mask and NTIA 01-43 protection levels are shown in Fig. 16. The SLiMS emissions levels are more than 55 dB below the NTIA 01-43 protection levels. The measured emissions are 3 dB or more below the UWB emissions mask.

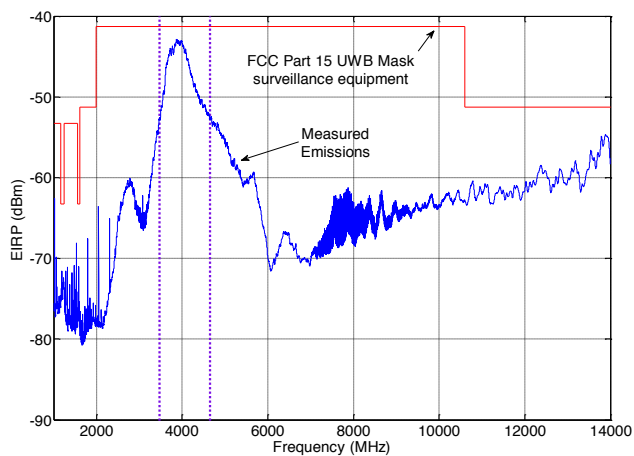


Fig. 15. A comparison of ITS measurements (RBW = 1.0 MHz and average detection) and the FCC Part15 UWB mask for surveillance equipment.

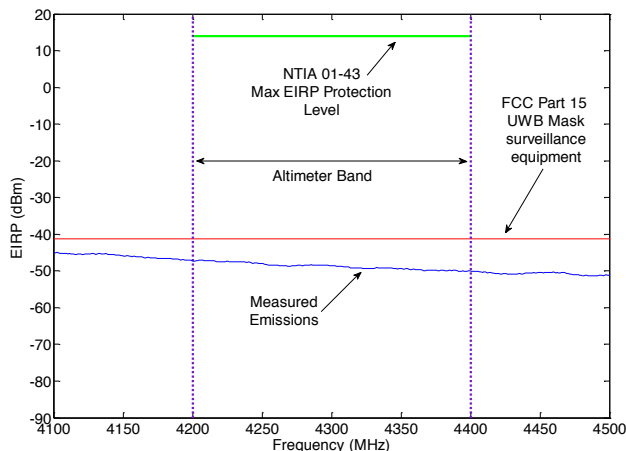


Fig. 16. A comparison of ITS measurements (RBW = 1.0 MHz and average detection) with the FCC UWB mask for surveillance equipment in the 4100–4500 MHz band and the NTIA 01-43 protection levels.

We should emphasize that the emission levels from the SLiMS system are quite low. As we have already described, a

combination of an anechoic chamber, sensitive measurement equipment, and precision positioning equipment are required to detect and quantify these UWB emissions. It is unlikely that SLiMS emissions could be measured to any degree of accuracy in any other environment, since noise and ambient interference would swamp out the emissions below the UWB emissions mask.

X. CONCLUSIONS

The measurement of the SLiMS UWB emissions places stringent demands on the measurement test setup and configurations. The design of a test setup for measuring this UWB radar first requires a thorough understanding of the time-domain characteristics of the emitted waveform. Once those are characterized and understood, we can progress into a customized regimen of swept-frequency measurements using a spectrum analyzer.

The main challenge we face is the low emissions levels, which has two ramifications. First, we need to use a fully anechoic chamber with a high level of isolation from RF ambients. Second, we need high-precision measurement and positioning equipment to accurately characterize the UWB emissions and pattern characteristics. In short, a high level of precision and expertise is required to perform the characterization of a device like SLiMS.

REFERENCES

- [1] R.T. Johnk, F.H. Sanders, K.E. Davis, G.A. Sanders, J.D. Ewan, R.L. Carey, S.J. Gunderson, “Conducted and radiated emissions measurements of an ultrawideband surveillance radar,” NTIA Report 13-1491, November 2012.
- [2] Manual of Regulations and Procedures for Federal Radio Frequency Management, Washington D.C., National Telecommunications and Information Administration, May, 2011.
- [3] G. Breed, “A summary of FCC rules for ultra wideband communications,” *High-Frequency Electronics*, January 2005, pp. 42-4